CHEMISTRY OF MATERIALS

pubs.acs.org/cm

Article

Hydroxyapatite Nanocoating on Calcium Peroxide Microparticles for Sustained Oxygen Release

Daisuke Tomioka, Satoshi Fujita, Jürgen Groll, and Michiya Matsusaki*

Cite This: *Chem. Mater.* 2023, 35, 5378−5391

Read Online

ACCESS | Metrics & More | Article Recommendations | Supporting Information

ABSTRACT: In the tissue engineering field, cell death due to oxygen shortage is still a major challenge for the construction and transplantation of three-dimensional (3D) tissues. To address this problem, oxygen-releasing materials have attracted much attention in recent years. Although calcium peroxide (CaO_2) is one of the most common oxygen sources for these types of materials, limitations have also been reported concerning the burst release of oxygen after immersion in water. Herein, we introduce a new strategy to delay the oxygen release from CaO_2 microparticles through coating with a hydroxyapatite (HAp) layer (HAp-CaO_2) that serves as a diffusion barrier. Strikingly, this coating can be applied by simple immersion of CaO_2 microparticles in phosphate buffer (PB) solution. We demonstrate that gelatin hydrogels with embedded HAp-CaO_2 microparticles release oxygen for 10 days as compared to only 3 days for identical hydrogels including uncoated CaO_2 microparticles. In addition, we demonstrate that the sustained oxygen supply from these hydrogels shows a drastic improvement in cell proliferation under hypoxic conditions. Taken together, this study introduces an easy strategy for sustained oxygen release based on inorganic microparticle formation that can be applied to a broad range of biomaterials for the development of oxygen-releasing materials.

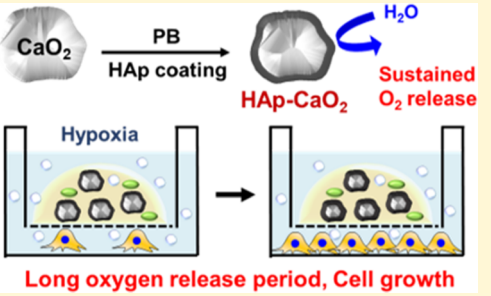

Downloaded via UNIV OF IOWA on December 18, 2023 at 15:27:31 (UTC).
See https://pubs.acs.org/sharingguidelines for options on how to legitimately share published articles.

1. INTRODUCTION

Regenerative medicine is a new medical technique for recovering tissue function by transplanting cells and tissues to the disease sites. However, before the angiogenesis to the transplanted tissues, insufficient oxygen supply results in cell death, preventing efficient tissue regeneration *in vivo*.[1,2] Moreover, *in vitro* construction of thick three-dimensional (3D) tissues is still a major challenge because limited diffusion of oxygen inside these tissues causes cell death.[3,4] Solving this oxygen shortage problem is therefore considered important for the development of regenerative medicine and tissue engineering.

To address the problem of cell death due to oxygen shortage, oxygen-releasing materials have attracted much attention in recent years.[5−7] Heme proteins such as hemoglobin[8,9] and myoglobin[10,11] are some of the most common oxygen sources for these materials because they supply oxygen in our body. However, the low payload of oxygen and protein stability are challenges, which prevent sustained oxygen supply. Although perfluorocarbons (PFCs) have also attracted much attention as an artificial oxygen carrier because of their high oxygen solubility,[12−14] the low payload of oxygen and the short duration of oxygen release are also challenges. To overcome these limitations, calcium peroxide (CaO_2) is often used for oxygen-releasing materials because CaO_2 can theoretically achieve a higher oxygen payload compared to heme proteins and PFC.[5] CaO_2 is an inorganic solid and it generates oxygen, hydrogen peroxide, and calcium hydroxide by the reaction with water.[15] Therefore, many researchers reported oxygen-releasing hydrogels by mixing CaO_2 into the hydrogels. However, the initial burst release of oxygen from CaO_2 is a major issue because of the uncontrollability of oxygen release after immersion in water.[16−19]

Recently, hydrophobic synthetic polymers such as poly(dimethylsiloxane),[20,21] poly(lactide-*co*-glycolide),[22] and polycaprolactone[23−25] have been used for the sustained oxygen release from CaO_2 by suppressing the reaction with water. Although sustained oxygen release of around 2 weeks was achieved in these reports, applications of these synthetic polymers for tissue engineering are somewhat limited due to their fabrication process.[26] Accordingly, sustained oxygen release from CaO_2 in water-rich materials such as hydrogels is strongly desired because hydrogels are widely used as cell scaffold materials. Furthermore, in the case of the hydrophobic polymer materials, CaO_2 is simply mixed in the polymer materials and thus the distribution of CaO_2 particles is totally random. Accordingly, some of the particles at the surface of the polymer materials easily contact with water to quickly produce oxygen. In other words, previously reported oxygen-releasing

Received: March 17, 2023
Revised: May 30, 2023
Published: July 3, 2023

ACS Publications

© 2023 American Chemical Society

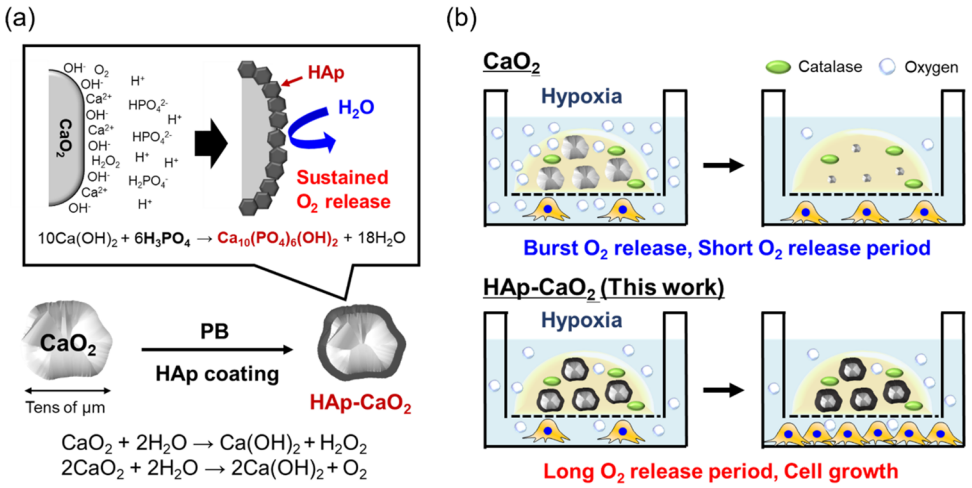

Figure 1. Schematic illustration of (a) the sustained oxygen release from CaO_2 microparticles through the HAp coating by PB treatment and (b) the sustained oxygen supply from the hydrogel including HAp-CaO_2 and catalase, which improved cell proliferation under a hypoxic condition.

materials are provided by simply mixing CaO_2 within the substrates such as hydrophobic synthetic polymers and hydrogels. To the best of our knowledge, there is no report about the surface modification of CaO_2 particles to achieve sustained oxygen release.

As a new strategy for the sustained oxygen release from CaO_2, we considered the surface modification of CaO_2 itself. Herein, we have achieved sustained oxygen release from CaO_2 microparticles by suppressing the reaction with water through the formation of hydroxyapatite (HAp) on the surface using a phosphate buffer (PB) (Figure 1a). It is known that the reaction between calcium hydroxide and phosphoric acid yields HAp which has poor solubility.[27,28] Thus, calcium hydroxide produced by the CaO_2 reaction is expected to react with phosphoric acid in PB to form HAp on the surface of CaO_2 microparticles. Since HAp is a main component of teeth and bones, this biocompatible surface modification will be preferable for tissue engineering applications, especially for hard tissues.[29−32] Furthermore, the HAp coating method consists of simply immersing CaO_2 in PB, indicating its applicability to existing and yet-to-be-developed oxygen-releasing materials. For general tissue engineering applications beyond hard tissue, oxygen-releasable gelatin hydrogels enzymatically cross-linked by transglutaminase (TG) were fabricated using catalase and CaO_2 microparticles coated with HAp (HAp-CaO_2). TG is an enzyme that cross-links the carboxamide groups of glutamine residue side chains with the primary amine of lysine residue side chains.[33] It is reported that TG-cross-linked gelatin hydrogels show excellent biocompatibility, and they have been applied to scaffolds for 3D cell culture,[34] 3D bioprinting,[35] and microsphere fabrication.[36,37] In addition, catalase has been incorporated in oxygen-releasable gelatin hydrogels because it is an enzyme that decomposes hydrogen peroxide into oxygen and water.[38] Therefore, the suppression of cytotoxicity derived from hydrogen peroxide is expected. Our results demonstrated that the sustained oxygen release from hydrogels including HAp-CaO_2 improved cell proliferation of various cell types under a hypoxic condition (Figure 1b). The developed oxygen-releasing hydrogels including HAp-CaO_2 therefore show great potential for solving the oxygen shortage problem in regenerative medicine and tissue engineering fields. In addition, our HAp-CaO_2 is expected to be applied for oxygen-releasing materials as a new oxygen source capable of sustained oxygen release.

2. EXPERIMENTAL SECTION

2.1. Materials. Calcium peroxide (CaO_2) (particle size <200 mesh (74 μm)), HEPES sodium salt, catalase from bovine liver, bovine serum albumin (BSA, A3294), collagenase from clostridium histolyticum (type I, C0130), fibronectin human plasma and Triton X-100 were purchased from Sigma-Aldrich (MO). Sodium dihydrogenphosphate, disodium hydrogenphosphate 12-water, gelatin (077-03155), calcium chloride anhydrous, 5 mol L^{-1} hydrochloric acid (HCl), sulfuric acid and trypsin from porcine pancreas were purchased from FUJIFILM Wako Pure Chemical Corporation (Osaka, Japan). Mineral oil high sensitivity (oxygen barrier oil) and Phalloidin-iFluor 594 Reagent were purchased from Abcam (Cambridge, U.K.). L(+)-ascorbic acid, potassium dihydrogenphosphate, Dulbecco's modified Eagle medium (DMEM) (transparent; 08489-45, cell culture; 08458-16), ethanol, Dulbecco's phosphate buffered saline (PBS), and 10% formaldehyde neutral buffer solution were purchased from Nacalai Tesque (Kyoto, Japan). Ammonium molybdate 4-hydrate was purchased from Kishida Chemical Co., Ltd. (Osaka, Japan). Transglutaminase (TG) was kindly donated by Ajinomoto Co., Inc. (Tokyo, Japan). Tert-butyl alcohol was purchased from Tokyo Chemical Industry Co., Ltd. (Tokyo, Japan). Fetal bovine serum (FBS) (10270), antibiotics (50 U mL^{-1} penicillin and 50 μg mL^{-1} streptomycin), and 4′,6-diamidino-2-phenylindole (DAPI) were purchased from Thermo Fisher Scientific (MA). Normal human dermal fibroblasts (NHDF, CC-2509) and human mesenchymal stem cells (MSC, PT-2501) were purchased from LONZA (Basel, Switzerland). HepG2 hepatocellular carcinoma cells (Human) were purchased from Cellular Engineering Technologies (HEPG2−500, IA). Normal goat serum was purchased from Jackson Immuno Research Laboratories Inc. (PA).

2.2. Oxygen Release Behavior of CaO_2 in Several Buffers. PB was prepared by mixing the same concentration of sodium dihydrogenphosphate solution and disodium hydrogenphosphate solution to adjust the solution pH to 7.0. The oxygen-releasing behavior of CaO_2 microparticles was determined by measuring the dissolved oxygen concentration in several buffers using a multi-parameter DO meter (HANNA, Woonsocket). 10 mg of CaO_2 was dispersed in 10 mL of HEPES (100 mM) and PB (25, 100, and 500 mM) in a sample tube. Next, the DO meter was immersed in the solution. To suppress the diffusion of oxygen to air, the sample solution and DO meter were fully covered by oxygen barrier oil. Dissolved oxygen concentration was measured at 37 °C every 2 min while stirring the solution.

https://doi.org/10.1021/acs.chemmater.3c00601
Chem. Mater. 2023, 35, 5378−5391

2.3. Dissolution Behavior of CaO_2 in Several Buffers. 10 mg of CaO_2 was placed in a sample tube. The movies for the dissolution behavior of CaO_2 microparticles were taken until 3 min after the addition of 10 mL of HEPES (100 mM) and PB (100 mM) to the sample tube.

2.4. Hydrogen Peroxide Release Behavior of CaO_2 in Several Buffers. 5 mg of CaO_2 was dispersed in 5 mL of HEPES (100 mM) and PB (100 mM). After 1 h of incubation at 37 °C, hydrogen peroxide concentration in each solution was quantified using an Oxiselect Hydrogen Peroxide/Peroxidase Assay Kit (Fluorometric) (STA-344, Cell Biolabs Inc., San Diego) according to the manufacturer's protocol. Due to the limitation of the detection range for this assay kit, supernatants of each sample were diluted 1000 times using an assay buffer. 50 μL of the sample solution was mixed with 50 μL of the working solution of the assay kit in a black 96-well plate (3603, Corning, NY). After 30 min incubation at room temperature, fluorescent intensity was measured by a microplate reader (SYNERGY/HTX multimode reader, BioTek Instruments, Winooski) using λ_{ex} = 540 nm for excitation wavelengths and λ_{em} = 590 nm for emission wavelengths. Hydrogen peroxide concentration was calculated from a standard curve obtained from the fluorescent intensities of the known concentrations of hydrogen peroxide (0−12.5 μM).

2.5. Characterization of the HAp Coating on CaO_2. The surface structure of uncoated CaO_2 and CaO_2 immersed in PB was analyzed by SEM and EDX measurements. CaO_2 was immersed in 100 and 500 mM PB at a concentration of 5 mg mL^{-1} for 1 h at 37 °C. The resulting samples were collected by centrifugation at 4000 rpm for 3 min and then washed three times by MilliQ. Samples were then dried under reduced pressure at 80 °C. For the high-resolution SEM, uncoated CaO_2 and CaO_2 immersed in PB were sputter-coated with osmium using an HPC-30 Plasma Coater (Vacuum Device, Ibaraki, Japan), and their surface morphologies were observed by a JSM-6701F instrument (JEOL Ltd., Tokyo, Japan). In the case of the dimension of the HAp layer, HAp-CaO_2 was crushed by a spatula before sputter-coating with osmium. For the elemental analysis on their surface, SEM-EDX measurements were performed by a Miniscope TM 3000 equipped with a Swift ED 3000 (Hitachi Ltd., Tokyo, Japan) without sputtering. Crystal structures of each sample were evaluated by XRD (AERIS, Malvern Panalytical, Malvern, U.K.), and chemical structures were evaluated by FT-IR (FT-720, HORIBA, Kyoto, Japan).

2.6. Characterization of the Cross-Section of the HAp-CaO_2 Plate. A CaO_2 plate was prepared by compressing CaO_2 microparticles at 30 MPa in a silicon sheet mold with a 6 mm diameter using a high-pressure jack (1-1187-01, As One, Osaka, Japan). The prepared CaO_2 plate was immersed in 500 mM PB for 1 h at 37 °C. After washing three times by MilliQ, the plate was dried under reduced pressure at 80 °C. Cross-sections of the prepared plate were analyzed by SEM-EDX measurements.

2.7. Quantitative Evaluation of Phosphorus Amount on CaO_2 by PB Treatment. The amount of phosphorus in CaO_2 was quantitatively evaluated using the molybdenum blue method as previously reported.[39,40] HAp-CaO_2 was prepared by immersing 3 mg of CaO_2 in 3 mL of 100 and 500 mM PB (1 mg mL^{-1}) for 1 h at 37 °C. After washing three times by MilliQ, HAp-CaO_2 was completely dissolved in 3 mL of 1 N HCl for 1 h. As a control sample, 3 mg of uncoated CaO_2 was also dissolved in 3 mL of 1 N HCl. To adjust the HCl concentration to 0.5 N, 3 mL of MilliQ was added to each sample. Due to the limitation of the detection range for this molybdenum blue method, the prepared samples were diluted 10 times using 0.5 N HCl. 250 μL of diluted sample solutions were mixed with 750 μL of the coloring reagent, consisting of 1 part of 10% ascorbic acid solution and 6 parts of 0.42% ammonium molybdate solution in 1 N H_2SO_4. The coloring reagent needs to be freshly prepared immediately before use. After 20 min of incubation in a water bath at 45 °C, the absorbance at 820 nm was measured using a UV−vis spectrophotometer (V-670M, JASCO, Tokyo, Japan). The standard curves were prepared using potassium dihydrogenphosphate in the same way. HAp concentrations were calculated assuming that all detected phosphorus was derived from HAp.

2.8. Fabrication of Oxygen-Releasing Hydrogels. For the hydrogel preparation, a 100 U mL^{-1} TG solution and 10 000 U mL^{-1} catalase solution were prepared using transparent DMEM, and a 0.5 M $CaCl_2$ solution was prepared using MilliQ. To prepare a gelatin stock solution, 2500 mg of gelatin was dissolved in 10 mL of transparent DMEM (20 wt %) by heating. HAp-CaO_2 was prepared by immersing 1 mg mL^{-1} CaO_2 in 100 and 500 mM PB for 1 h at 37 °C. The resulting HAp-CaO_2 were collected by centrifugation at 4000 rpm for 3 min. Uncoated CaO_2 or HAp-CaO_2 were dispersed in a gelatin stock solution, and then 10 000 U mL^{-1} catalase, 100 U mL^{-1} TG, 0.5 M $CaCl_2$, and transparent DMEM were mixed so that the final concentrations were 2.5, 10 mg mL^{-1} CaO_2, 16 wt % gelatin, 10 U mL^{-1} TG, 100 U mL^{-1} catalase, and 2.5 mM $CaCl_2$, respectively. HAp-CaO_2 concentration was defined from the CaO_2 concentration before the HAp coating. The samples without catalase were prepared in the same way. For the evaluation of hydrogel formation, 800 μL of the prepared solutions were added to the sample tube. After 1 h incubation at 37 °C, gelation was checked by tilting the sample tube.

2.9. Characterization of the Porous Structure of Oxygen-Releasing Hydrogels. Porous structures of hydrogels were characterized by SEM. 200 μL of hydrogels with catalase including 2.5 mg mL^{-1} different types of CaO_2 (uncoated CaO_2, HAp-CaO_2 (100 and 500 mM PB)) were prepared in a 24-well plate insert (3470, Corning, NY). As a control, a hydrogel without CaO_2 was fabricated in the same way. To suppress the shrinkage of the hydrogels during the lyophilization procedure, t-butyl alcohol substitution was performed before the lyophilization. Briefly, the prepared hydrogels were immersed in ethanol for 1 h and then immersed in *t*-butyl alcohol 3 times for 1 h. After lyophilization and cutting the samples, surface morphologies of each of the samples sputter-coated with osmium were observed by SEM.

2.10. Compression Test of Oxygen-Releasing Hydrogels. Mechanical properties of hydrogels were characterized by a compression test using EZTest (SHIMADZU, Kyoto, Japan). 200 μL of hydrogels with catalase including 0 and 2.5 mg mL^{-1} HAp-CaO_2 (500 mM PB) were prepared in a 24-well plate insert. Hydrogels were taken out from the insert and the compression test was performed at a constant test speed of 0.5 mm min^{-1}. The Young modulus of hydrogels was calculated from the slope of the stress−strain curve between 10 and 20% strains.

2.11. Rheological Test of Oxygen-Releasing Hydrogels. The rheological properties of hydrogels were characterized by a rheometer (MCR302, Anton Paar, Graz, Austria). 200 μL of hydrogels with catalase including 0 and 2.5 mg mL^{-1} HAp-CaO_2 (500 mM PB) were prepared in a 24-well plate insert. Hydrogels were taken out from the insert and then dynamic frequency sweeps were performed from 0.1 to 10 rad s^{-1} at 1.0% strain amplitude. The starting axial force for all measurements was 0.2 N.

2.12. Swelling Behavior of Oxygen-Releasing Hydrogels. 200 μL of hydrogels with catalase including 0 and 2.5 mg mL^{-1} HAp-CaO_2 (500 mM PB) were prepared in a 24-well plate insert. To study the swelling behaviors of hydrogels, hydrogels were incubated in 2 mL of DMEM for 1 day at 37 °C. After measuring the swollen weight, hydrogels were freeze-dried, and then dry weights were also measured. The weight-swelling ratio was calculated as the ratio of the swollen weight to the dry weight of hydrogels.

2.13. Degradation Behavior of Oxygen-Releasing Hydrogels. 200 μL of hydrogels with catalase including 0 and 2.5 mg mL^{-1} HAp-CaO_2 (500 mM PB) were prepared in a 24-well plate insert. Prepared hydrogels were freeze-dried and then dry weights (W_0) were measured. To study the degradation behaviors of hydrogels, prepared hydrogels were incubated in 2 mL of DMEM at 37 °C. After 7 and 14 days of incubation, hydrogels were freeze-dried, and then dry weights (W_t) were measured. The remaining mass ratio of hydrogels was calculated as W_t/W_0.

2.14. Hydrogen Peroxide Release from Oxygen-Releasing Hydrogels. Hydrogen peroxide concentrations in transparent DMEM including hydrogels were evaluated using an Oxiselect

https://doi.org/10.1021/acs.chemmater.3c00601
Chem. Mater. 2023, 35, 5378−5391

Hydrogen Peroxide/Peroxidase Assay Kit. 200 μL of hydrogels with or without catalase including different concentrations of HAp-CaO_2 (100 mM PB) (0, 2.5, 5, 10 mg mL^{-1}) were incubated with 2 mL of transparent DMEM in a 24-well plate (3820-024, IWAKI, Shizuoka, Japan) at 37 °C in a 5% CO_2 incubator. After 3 days of incubation, 100 μL of the supernatant of each sample was collected. Due to the limitation of the detection range for the hydrogen peroxide assay kit, the supernatant derived from hydrogel including 10 mg mL^{-1} HAp-CaO_2 without catalase was diluted 100 times, and hydrogel including 5 mg mL^{-1} HAp-CaO_2 without catalase was diluted 10 times. The hydrogen peroxide concentration of each sample was evaluated as mentioned above.

2.15. pH Measurement of DMEM with Oxygen-Releasing Hydrogels. Changes in pH in transparent DMEM including hydrogels were evaluated. 200 μL of hydrogels with catalase including different concentrations of HAp-CaO_2 (100 mM PB) (0, 2.5, 5, 10 mg mL^{-1}) were incubated with 2 mL of transparent DMEM in a 24-well plate at 37 °C in a 5% CO_2 incubator. After 1 h, 1, 2, 3, and 5 days of incubation, the pH in 100 μL of the supernatant of each sample was measured using a pH meter (LAQUAtwin-pH-22B, HORIBA, Kyoto, Japan). After each pH measurement, 100 μL of transparent DMEM was added to each sample.

2.16. Oxygen Release Behavior of Hydrogels. To evaluate the oxygen release behavior of hydrogels, the dissolved oxygen amount in DMEM including hydrogels was measured under a hypoxic condition using an SDR SensorDish Reader (SDRSensorDishReader, PreSens, Regensburg, Germany). 200 μL of hydrogels with catalase including different concentrations and types of CaO_2 (2.5 mg mL^{-1} uncoated CaO_2, 2.5 mg mL^{-1} HAp-CaO_2 (100 mM PB), and 2.5, 5, and 10 mg mL^{-1} HAp-CaO_2 (500 mM PB)) were fabricated in a 24-well plate insert as mentioned above. As a control, the hydrogel without CaO_2 was fabricated in the same way. 24-well plate inserts were put in a 24-well sensor dish (OxoDishOD24, PreSens, Regensburg, Germany) and then 2 mL of transparent DMEM was added to each sample. As a control, DMEM without hydrogels was also prepared. The SensorDish Reader and the 24-well sensor dish were placed in a hypoxia cell culture airtight bag (6−8669−03, As one, Osaka, Japan). To create a hypoxic condition, three anaeropack O_2 absorbers (Mitsubishi Gas Chemical Company Inc., Tokyo, Japan) were added to the bag and it was then completely sealed using parafilm. The dissolved oxygen amount in DMEM was then monitored at 37 °C after the first 6 h and for each of the 24 h.

2.17. Isolation of ADSC from Adipose Tissues. ADSC was isolated from adipose tissues using a previously reported method.[41] Abdominal human adipose tissues from patients were isolated at the Kyoto Prefectural University of Medicine Hospital and kept on an ice pack during transportation to Osaka University. The tissues were first washed in PBS containing 5% of antibiotics. Then, 8−10 g of tissue were separated into fragments to fill the 6 wells of a 6-well plate and then minced to obtain a size of around 1 mm^3 using autoclaved scissors and tweezers directly in 2 mL of collagenase solution at 2 mg mL^{-1} in DMEM 0% FBS, 5% BSA and 1% antibiotics (sterilized by filtration). After 1 h of incubation at 37 °C with 250 rpm rotation, DMEM was added and the lysate was filtrated using a 500 μm filter before being centrifuged for 3 min at 80*g*. The cell pellet was washed twice in PBS with 5% BSA and 1% antibiotics and once in complete DMEM, with 3 min of centrifugation at 80*g* between each wash. Then, the final pellet was resuspended in DMEM for ADSC expansion by changing the medium every day for 3 days and then passaging the cells when they reached 80% of confluency.

2.18. Cell Culture with Oxygen-Releasing Hydrogels Under a Hypoxic Condition. Cell proliferation under a hypoxic condition with oxygen-releasing hydrogels was evaluated by a WST-8 (CCK-8) kit assay. Briefly, 200 μL of hydrogels with catalase including different concentrations of HAp-CaO_2 (500 mM PB) (0, 2.5, 5, 10 mg mL^{-1}) were fabricated in a 24-well plate insert and washed 3 times with 2 mL of DMEM containing 10% FBS and 1% antibiotics. 2×10^4 cells of NHDF, MSC, ADSC, and HepG2 were seeded on a 24-well plate using 1 mL of DMEM containing 10% FBS and 1% antibiotics. After 3 h incubation at 37 °C in a 5% CO_2 incubator, the 24-well plate inserts containing hydrogels were placed in the 24-well plate and then 1 mL of DMEM containing 10% FBS and 1% antibiotics was added. As a control, a cell culture without hydrogels was also prepared. The 24-well plates were incubated in a gas barrier box (As One, GB-3.0L, Osaka, Japan) with two anaeropack O_2 absorbers at 37 °C to create a hypoxic condition. The WST assay reagent was prepared by mixing transparent DMEM and cell count reagent SF (Nacalai Tesque, Kyoto, Japan) at a ratio of 9:1. After 7 days of incubation under a hypoxic condition, cells were washed with 1 mL of PBS and then 200 μL of the WST assay reagent was added. The cells were incubated in a 5% CO_2 incubator for 1 h for NHDF and 45 min for MSC, ADSC, and HepG2 at 37 °C. Then, 100 μL of WST solutions from each well were collected in a 96-well plate Transwell (3860-096, IWAKI, Shizuoka, Japan), and absorbance at 450 nm was measured using a microplate reader. The mitochondrial activity of each sample was standardized from the relative values of absorbance at 450 nm as compared to 100% for that of a cell culture without a hydrogel. Phase contrast images of each sample were also taken using an EVOS XL Core Imaging System (Thermo Fisher Scientific, MA) after 7 days of cell culture.

2.19. Cell Culture Using Preincubated Oxygen-Releasing Hydrogels. Cell proliferation under a hypoxic condition using preincubated oxygen-releasing hydrogels was also evaluated by the WST-8 kit assay. 200 μL of hydrogels with catalase including different concentrations and types of CaO_2 (2.5 mg mL^{-1} uncoated CaO_2, 0, 2.5, 5, 10 mg mL^{-1} HAp-CaO_2 (500 mM PB)) were fabricated in a 24-well plate insert and then incubated in 2 mL of DMEM containing 10% FBS and 1% antibiotics for 3 days in a 5% CO_2 incubator. Next, 2×10^4 cells of NHDF were cultured in a 24-well plate with hydrogels in the 24-well plate insert under a hypoxic condition as mentioned above. After 7 days of cell culture, the WST assay was performed for 45 min incubation as mentioned above.

2.20. Long-Term Cell Culture Using Oxygen-Releasing Hydrogels. For the long-term cell culture using oxygen-releasing hydrogels, 2×10^4 cells of NHDF were cultured in a 24-well plate using 2 mL of DMEM containing 10% FBS and 1% antibiotics with 200 μL of hydrogels including 10 mg mL^{-1} HAp-CaO_2 (500 mM PB) in a 24-well plate insert under a hypoxic condition as mentioned above. After 7 days of incubation at 37 °C, the culture medium was exchanged for a fresh one and then hydrogels were removed or retained. After an additional 7 days of cell culture under a hypoxic condition, the cells were washed with PBS and then incubated with a 0.1% trypsin solution (PBS) for 5 min at 37 °C. The living cell number of detached cells was evaluated by a trypan blue solution and a Countess II automated cell counter (Thermo Fisher Scientific, MA). As a control, the living cell number after 7 days of cell culture with hydrogels under a hypoxic condition was evaluated in the same way.

2.21. Construction of the 3D Tissue in the Presence of the Oxygen-Releasing Hydrogel. For the construction of the 3D tissue in the presence of an oxygen-releasing hydrogel, 1 mL of 16 wt % gelatin solution (DMEM) containing 10 U mL^{-1} TG, 100 U mL^{-1} catalase, 2.5 mM $CaCl_2$, and 2.5 mg mL^{-1} HAp-CaO_2 (500 mM PB) was added in the 24-well plates. Before the gelation, a 24-well insert containing 100 μL of 0.2 mg mL^{-1} fibronectin solution (50 mM Tris buffer at pH 7.4) was put in the gelatin solution. After 1 h of incubation at 37 °C for the gelation, the fibronectin solution was removed and the obtained hydrogel was washed with culture medium (DMEM containing 10% FBS and 1% antibiotics). 5×10^6 cells of L929 were suspended in 200 μL of culture medium and added to the 24-well insert. 400 μL of culture medium was also added in the 24-well plate. After 15 min of centrifugation of the 24-well plate at 1100 rpm, 1 mL of culture medium was added. As a control sample, the L929 tissue was constructed in the 24-well insert using the same procedure without hydrogels. Tissues were cultured in the 5% CO_2 incubator and culture medium was exchanged every day. After 3 days of culture, the L929 tissues were fixed with a 10% formaldehyde neutral buffer solution. For histology staining and fluorescence imaging, the fixed 3D tissues were sent to the Applied Research Company for paraffin embedding. Sectioned 3D tissues were stained with hematoxylin−eosin (HE) staining. The images were captured

https://doi.org/10.1021/acs.chemmater.3c00601
Chem. Mater. 2023, 35, 5378−5391

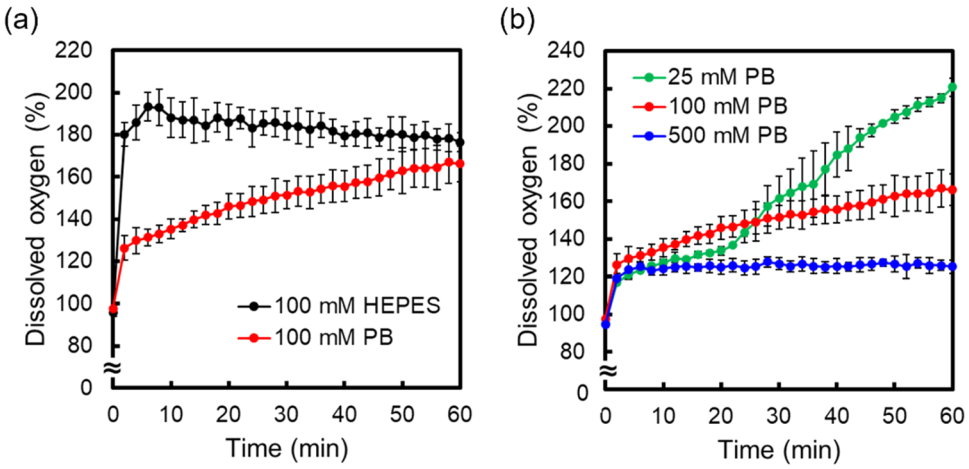

Figure 2. Dissolved oxygen changes in (a) 100 mM HEPES and 100 mM PB and (b) 25, 100, and 500 mM PB for 1 h at 37 °C in a closed system after the addition of 1 mg mL^{-1} CaO_2. All data are representative of three independent experiments.

using an FL EVOS Auto microscope (Thermo Fisher Scientific, MA). For the calculation of cell density in the HE staining images, cell numbers in the five areas (200 μm × 200 μm) around the center area were counted per each tissue by ImageJ. For the fluorescence imaging, the nuclei were stained with DAPI, and F-actin was detected by phalloidin. Sectioned 3D tissues were permeabilized with 0.3% Triton X-100 for 5 min and blocked with 1% bovine serum albumin and 10% normal goat serum in PBS. The tissues were then incubated with a staining solution (Phalloidin-iFluor 594, DAPI, 1:500 dilution in PBS). After washing with PBS, the 3D tissue was finally observed using a confocal laser scanning microscope (CSLM) FluoView FV3000 (Olympus, Tokyo, Japan). The images were taken by keeping the same exposure time and excitation power for each sample.

2.22. Ethics Statement. The adipose tissues were collected from the Kyoto Prefectural University of Medicine Hospital (Kyoto, Japan) after abdominal adipose tissues or liposuction isolation of human female donors. All use was approved by the Human Ethics Committee (Approval number: ERB-C-1317-1) of the Kyoto Prefectural University of Medicine Institutional Review Board and conformed to the principles outlined in the Declaration of Helsinki.

2.23. Statistical Analysis. In this study, three independent experiments were carried out for each experiment, and the results are expressed as the mean ± SD. Error bars represent standard deviations. For statistical analyses, Student's *t*-tests were performed to assess the variance. *p*-values <0.05 were considered statistically significant.

3. RESULTS AND DISCUSSION

3.1. Oxygen Release Behavior of CaO_2 Microparticles in Several Buffers. The chemical reaction between CaO_2 and water is as follows:[15]

$$2CaO_2 + 2H_2O \rightarrow 2Ca(OH)_2 + O_2$$

$$CaO_2 + 2H_2O \rightarrow Ca(OH)_2 + H_2O_2$$

As shown in Figure 1b, the rapid reaction between CaO_2 and water results in a burst release of oxygen in the solution. On the other hand, sustained oxygen release from CaO_2 is expected in PB through the formation of HAp on the surface because the reaction between calcium hydroxide and phosphoric acid provides HAp as follows:[27,28]

$$10Ca(OH)_2 + 6H_3PO_4 \rightarrow Ca_{10}(PO_4)_6(OH)_2 + 18H_2O$$

To confirm this hypothesis, oxygen release behaviors of CaO_2 microparticles (particle size <74 μm) were evaluated in 4-(2-hydroxyethyl)piperazine-1-ethanesulfonic acid (HEPES) buffer (pH 7.4) and PB (pH 7.0). HEPES is known as an effective buffer for culturing tissues and cells *in vitro* and is often used in the field of biochemistry as well. Dissolved oxygen (DO) concentration was measured by immersing a DO meter in each buffer after the addition of CaO_2 at a concentration of 1 mg mL^{-1}. To prevent the diffusion of oxygen into air, the buffer and DO meter were fully covered by oxygen barrier oil. In the case of 100 mM HEPES, the dissolved oxygen concentration increased to 200% within 6 min and then maintained the same value (Figure 2a). Furthermore, after the addition of CaO_2 in HEPES, CaO_2 disappeared within 3 min (Movie S1). These results suggest that the reaction between CaO_2 and water was completed quickly in HEPES. On the other hand, the initial burst increase of dissolved oxygen concentration was dramatically suppressed in 100 mM PB (Figure 2a). Furthermore, white solids remained in the solution after the addition of CaO_2 in 100 mM PB (Movie S2). We also evaluated hydrogen peroxide release from CaO_2 in each buffer (Figure S1). As with oxygen, hydrogen peroxide release from CaO_2 was dramatically suppressed in PB compared to HEPES. These results suggest that the reaction between CaO_2 and water was suppressed in PB, probably because HAp formation on CaO_2 delays this reaction. We hypothesize that the formed HAp layer acts as a diffusion barrier to water, thus significantly slowing down the reaction of water with CaO_2 and thus also subsequent oxygen formation.

To evaluate the effect of PB concentration on the oxygen release behavior of CaO_2, the dissolved oxygen concentration was measured in 25, 100, and 500 mM PB in the same way (Figure 2b). Interestingly, as the PB concentration increased from 25 to 100 and 500 mM, the dissolved oxygen concentration after 1 h of incubation decreased from 220 to 160 and 120%. According to these results, the reaction between CaO_2 and water was suppressed especially at higher PB concentrations, probably because the amount of HAp on CaO_2 also increased with PB concentration. The observed behavior fits our hypothesis, as the diffusion length of water through the HAp layer is increased with growing layer thickness, thus slowing down the oxygen production with increasing layer thickness. Since the dissolved oxygen amount in 500 mM PB has plateaued within 1 h at 37 °C, HAp-CaO_2 was prepared by immersing CaO_2 in PB for 1 h at 37 °C for further studies.

https://doi.org/10.1021/acs.chemmater.3c00601
Chem. Mater. 2023, 35, 5378−5391

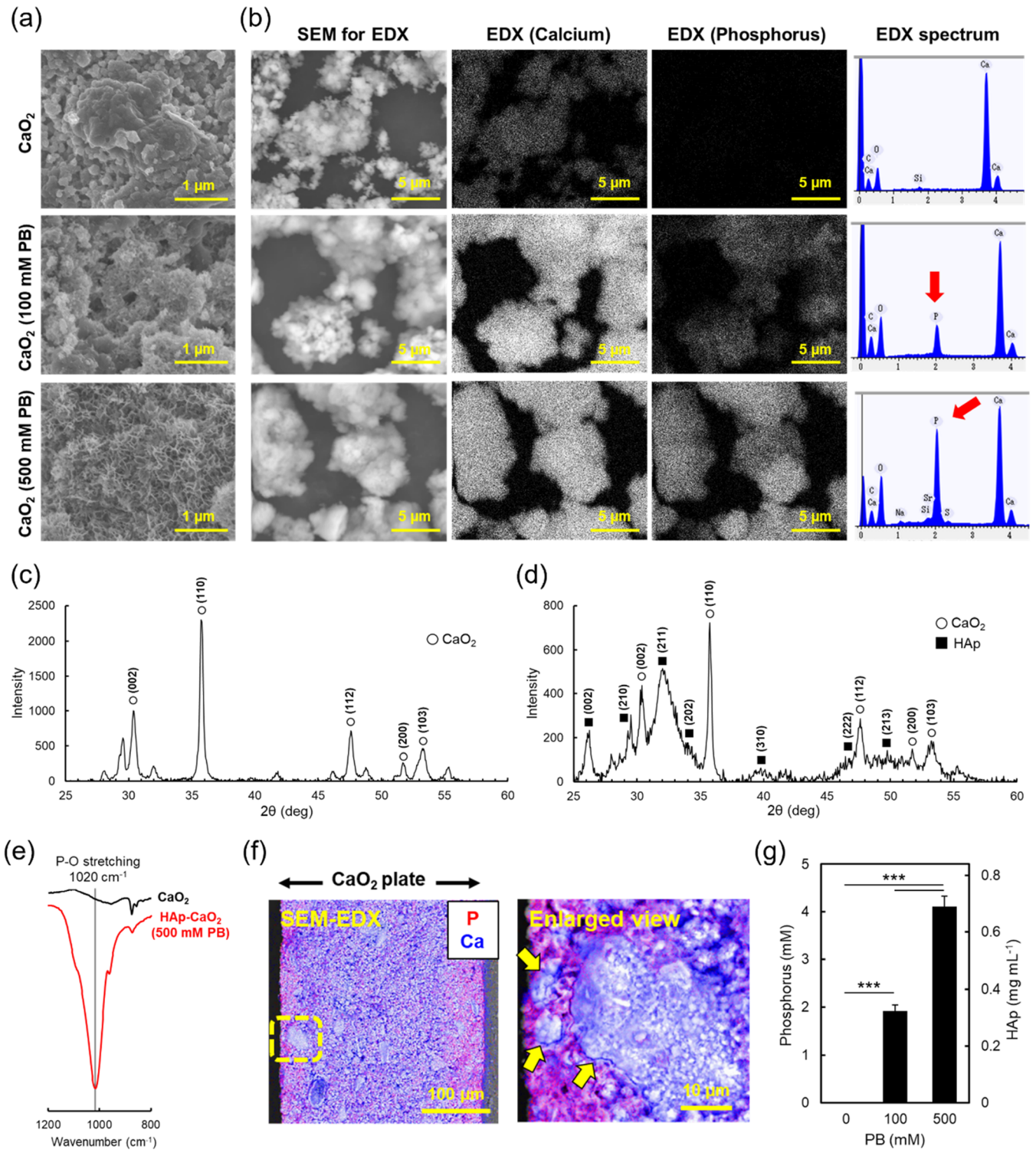

Figure 3. Characterization of the HAp coating on CaO_2 microparticles. (a) SEM images and (b) elemental mapping of calcium and phosphorus, and the EDX spectrum of CaO_2 (top) and CaO_2 immersed in 100 mM PB (middle) and 500 mM PB (bottom) for 1 h. The XRD spectrum of (c) CaO_2 and (d) CaO_2 immersed in 500 mM PB. (e) FT-IR spectrum of CaO_2 and CaO_2 immersed in 500 mM PB. (f) SEM and elemental mapping of calcium (blue) and phosphorus (red) of the cross-section of the CaO_2 plate after immersing the CaO_2 plate in 500 mM PB and enlarged view of the yellow area. (g) Phosphorus and HAp amount in CaO_2 and CaO_2 immersed in 100 and 500 mM PB. HAp concentrations were calculated assuming that all detected phosphorus was derived from HAp. The data are representative of three independent experiments, mean ± SD. ***$p <$ 0.001.

3.2. Characterization of HAp-CaO_2. To confirm the HAp coating on CaO_2 microparticles by PB treatment, the surface morphology of CaO_2 was evaluated. Figures 3a, S2, and S3 show scanning electron microscopy (SEM) images of untreated CaO_2 and CaO_2 immersed in 100 and 500 mM PB for 1 h at 37 °C. CaO_2 immersed in PB showed a porous structure on the surface, suggesting structural surface changes and the formation of the HAp nanocrystal.[30] In addition, SEM images

https://doi.org/10.1021/acs.chemmater.3c00601
Chem. Mater. 2023, 35, 5378−5391

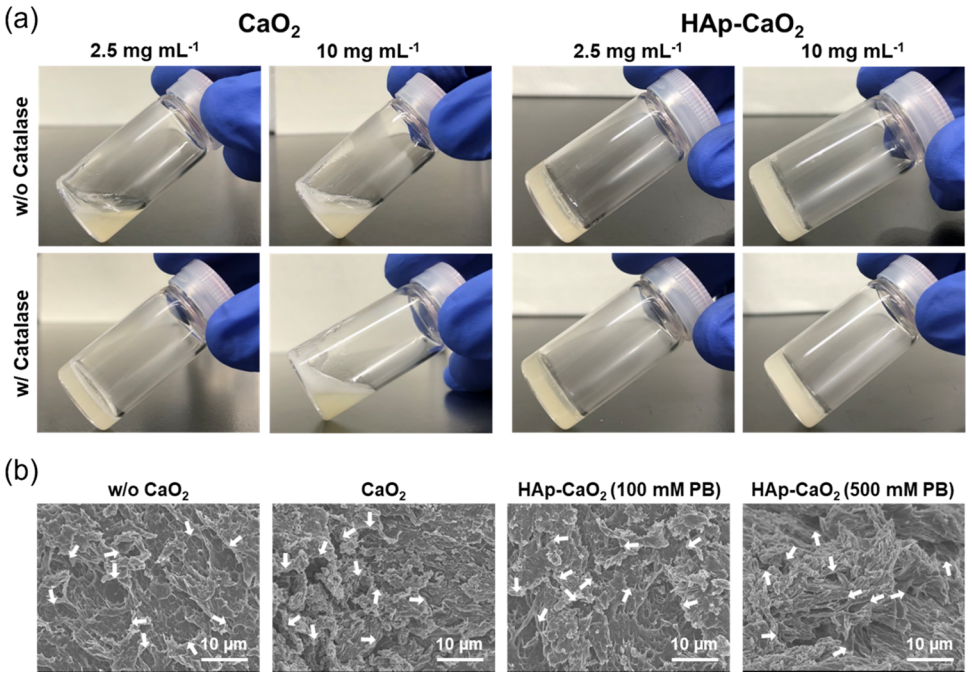

Figure 4. (a) Hydrogel formation after 1 h of incubation at 37 °C after mixing 16 wt % gelatin, 10 U mL^{-1} TG, 2.5 mM $CaCl_2$, 0 and 100 U mL^{-1} catalase, and various concentrations of CaO_2 or HAp-CaO_2 (100 mM PB). (b) SEM images of the hydrogels including 100 U mL^{-1} catalase and 0 and 2.5 mg mL^{-1} of CaO_2 or HAp-CaO_2 (100 and 500 mM PB) (white arrows indicate pores for the estimation of pore size). HAp-CaO_2 (100 and 500 mM PB) were prepared by immersing CaO_2 in 100 and 500 mM PB for 1 h.

of the dimensions of the HAp layer also showed the same porous structure (Figure S4). After the PB treatment of CaO_2, the particle size of CaO_2 microparticles was unchanged (Figure S5). For the elemental analysis on the surface of CaO_2, SEM and energy-dispersive X-ray spectroscopy (EDX) measurements were performed (Figure 3b). The elemental mapping of untreated CaO_2 showed calcium but no phosphorus at the same location of CaO_2 in the SEM image. On the other hand, CaO_2 immersed in 100 and 500 mM PB showed both calcium and phosphorus at the same location of CaO_2 in the SEM images. These results suggested that phosphorus-containing crystals were formed on the surface of CaO_2 by PB treatment.[31,32] Furthermore, the EDX spectra of each sample showed that the peak intensity derived from phosphorus increased with PB concentration (red arrow in the figure). Accordingly, it is also suggested that the amount of phosphorus-containing crystals on the surface of CaO_2 increased with PB concentration. It is known that the Ca/P ratio of HAp is 1.67.[30−32] The Ca/P ratio of HAp-CaO_2 was calculated as 4.62 and 1.62 for 100 and 500 mM PB, respectively. Because CaO_2 itself contained Ca, the Ca/P ratio at 100 mM PB conditions indicated a much higher value than the theoretical ratio of HAp. On the other hand, HAp-CaO_2 prepared by 500 mM PB showed a closer Ca/P ratio (1.62) of ideal HAp (1.67) probably due to the thicker HAp layer than the measurement depth of EDX. These results strongly support HAp coating on CaO_2 microparticles by PB treatment.

To clarify the crystal structure of phosphorus-containing crystals, X-ray diffraction (XRD) was measured (Figure 3c,d). In both untreated CaO_2 and CaO_2 immersed in 500 mM PB, peaks at 30, 36, 48, 52, and 53° were observed, which were assigned to the (002), (110), (112), (200), and (103) reflections of CaO_2.[42] Peaks at 26, 29, 32, 34, 40, 47, and 50° were also observed in CaO_2 immersed in 500 mM PB, which were assigned to the (002), (210), (211), (202), (310), (222), and (213) reflections of HAp.[43,44] According to the XRD data, phosphorus-containing crystals were identified as HAp. HAp formation was also confirmed using Fourier-transform infrared spectroscopy (FT-IR) (Figure 3e). The clear band at 1,020 cm^{-1} which was assigned to the P−O stretching vibration was observed in CaO_2 immersed in 500 mM PB, suggesting HAp formation.[31,44] According to these results, HAp coating on CaO_2 microparticles by PB treatment was confirmed, which enabled sustained oxygen release from CaO_2 in PB (Figure 2).

For the cross-section analysis of HAp-CaO_2, a CaO_2 plate was prepared by compressing CaO_2 microparticles using a mold. After immersing the CaO_2 plate in 500 mM PB for 1 h, SEM-EDX measurements of the cross-section of the CaO_2 plate were taken. As shown in the merged image of SEM and elemental mapping, calcium was observed throughout the cross-sections (Figure 3f). On the other hand, phosphorus was observed mainly near the plate surface, suggesting that HAp is formed on the surface of the CaO_2 plate. A small amount of phosphorus was also observed inside the CaO_2 plate, probably because of PB that penetrated through the voids of the CaO_2 plate to react with CaO_2 inside. Furthermore, according to the enlarged merged image of SEM and elemental mapping, phosphorus was observed on the surface of the CaO_2 microparticles in the plate and the thickness of the HAp layer on these microparticles was estimated to be no more than a few micrometers.

Since SEM-EDX measurements suggested PB concentration-dependent HAp formation, the amount of phosphorus on the surface of CaO_2 was quantitatively evaluated using the molybdenum blue method[39,40,45] (Figure 3g). HAp-CaO_2 was dissolved in 1 N HCl [$Ca_{10}(PO_4)_6(OH)_2 + 8H^+ \rightarrow 10Ca^{2+} + 6HPO_4^{2-} + 2H_2O$] and then the amount of dissolved phosphorus ions was measured. As expected, no phosphorus ions were detected in the case of untreated CaO_2. When 1 mg

https://doi.org/10.1021/acs.chemmater.3c00601
Chem. Mater. 2023, 35, 5378−5391

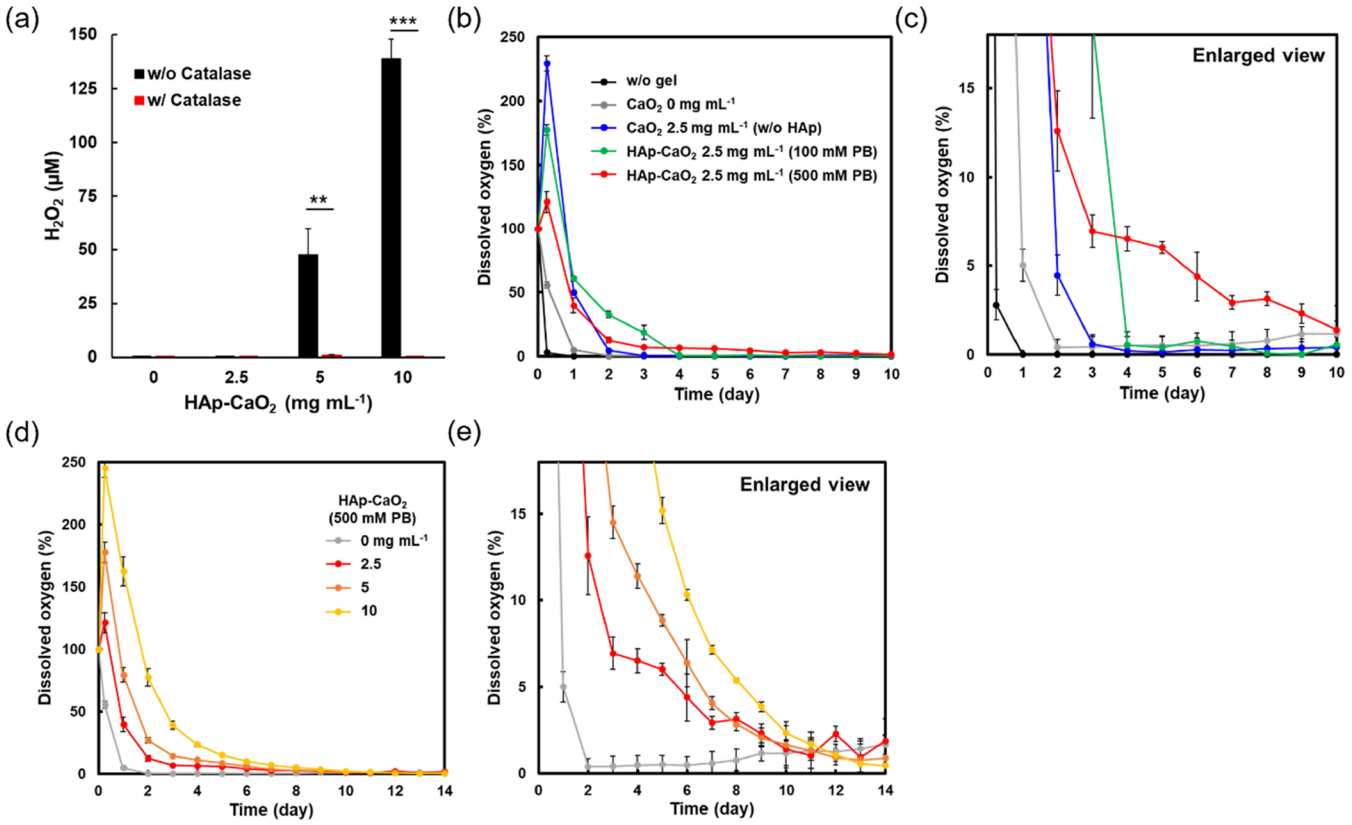

Figure 5. (a) Hydrogen peroxide concentrations in 2 mL of DMEM with 200 μL of hydrogels including 0 (black) and 100 U mL^{-1} (red) catalase and various concentrations of HAp-CaO_2 (100 mM PB) after 3 days incubation. Dissolved oxygen changes in 2 mL of DMEM with 200 μL of hydrogels including 100 U mL^{-1} catalase, (b, c) 0 and 2.5 mg mL^{-1} CaO_2 or HAp-CaO_2 (100 and 500 mM PB), and (d, e) 0, 2.5, 5, and 10 mg mL^{-1} HAp-CaO_2 (500 mM PB) under a hypoxic condition. Panels (c) and (e) show enlarged views of panels (b) and (d), respectively. All data are representative of three independent experiments, mean ± SD. $^{**}p < 0.01$ and $^{***}p < 0.001$.

mL^{-1} (13.84 mM) CaO_2 was immersed in 100 mM PB for 1 h, 1.92 mM of phosphorus ions was detected, which corresponds to 0.32 mg mL^{-1} HAp, assuming that all of the detected ions were derived from HAp. Furthermore, in the case of 500 mM PB, 4.10 mM phosphorus ions were detected, which corresponds to 0.69 mg mL^{-1} HAp. These results confirmed that the HAp amount on CaO_2 increased with PB concentration, which enabled PB concentration-dependent oxygen release from CaO_2 (Figure 2b).

3.3. Fabrication and Characterization of Oxygen-Releasing Hydrogels. For the broader application of HAp-CaO_2 to tissue engineering, we demonstrate that HAp-CaO_2 microparticles can be used as additives to hydrogels in the example of enzymatically cross-linked gelatin hydrogels. HAp-CaO_2 was prepared by immersing CaO_2 microparticles in 100 or 500 mM PB for 1 h at 37 °C. After mixing gelatin, TG, catalase, and CaO_2 or HAp-CaO_2 in Dulbecco's modified Eagle medium (DMEM), the sample solutions were incubated for 1 h at 37 °C to gelate (Figure 4a). Interestingly, in the case of uncoated CaO_2, gelation was not observed without catalase. It is reported that TG is deactivated by hydrogen peroxide due to conformational changes of the peptide main chain associated with disulfide bond formation.[46] Thus, it is suggested that cross-linking of gelatin by TG was suppressed without catalase because of the initial burst release of hydrogen peroxide from CaO_2. In addition, gelation was observed at 2.5 mg mL^{-1} CaO_2 but not at 10 mg mL^{-1} CaO_2 with catalase. This is probably because of the deactivation of TG by hydrogen peroxide prior to the decomposition by catalase at the higher concentration of uncoated CaO_2. On the other hand, gelation was observed in all samples using HAp-CaO_2 (100 mM PB) because the HAp coating on CaO_2 suppresses the burst release of hydrogen peroxide. These results clearly suggested that HAp-CaO_2 is applicable to the hydrogels obtained by enzymatic reactions, which are difficult to prepare using uncoated CaO_2. The morphology of freeze-dried hydrogels was analyzed by SEM (Figure 4b). Porous structures with pore sizes of around 5−10 μm were identified in all hydrogels, suggesting no marked differences in hydrogel structures. The compression tests and rheological tests showed that hydrogels with and without HAp-CaO_2 had similar strain−stress curves, Young's modulus, and storage modulus (G'), suggesting that these hydrogels have similar mechanical properties (Figure S6a−c). Swelling behaviors and degradation behaviors also showed similar trends between hydrogels with and without HAp-CaO_2 (Figure S6d,e). These results suggested that the incorporation of HAp-CaO_2 in the gelatin hydrogel enzymatically cross-linked by TG did not affect hydrogel properties.

When CaO_2 reacts with water, hydrogen peroxide is also released as a byproduct. Since this compound exhibits cytotoxic properties above certain concentrations, hydrogen peroxide release from hydrogels was evaluated in DMEM after 3 days of incubation (Figure 5a). In the case of hydrogels without catalase, the concentration of hydrogen peroxide increased with HAp-CaO_2 (100 mM PB) concentration (HAp-CaO_2 5 mg mL^{-1}, 47 μM; 10 mg mL^{-1}, 139 μM). However, hydrogen peroxide was not detected in the hydrogel including 2.5 mg mL^{-1} HAp-CaO_2, probably because the released

https://doi.org/10.1021/acs.chemmater.3c00601
Chem. Mater. 2023, 35, 5378−5391

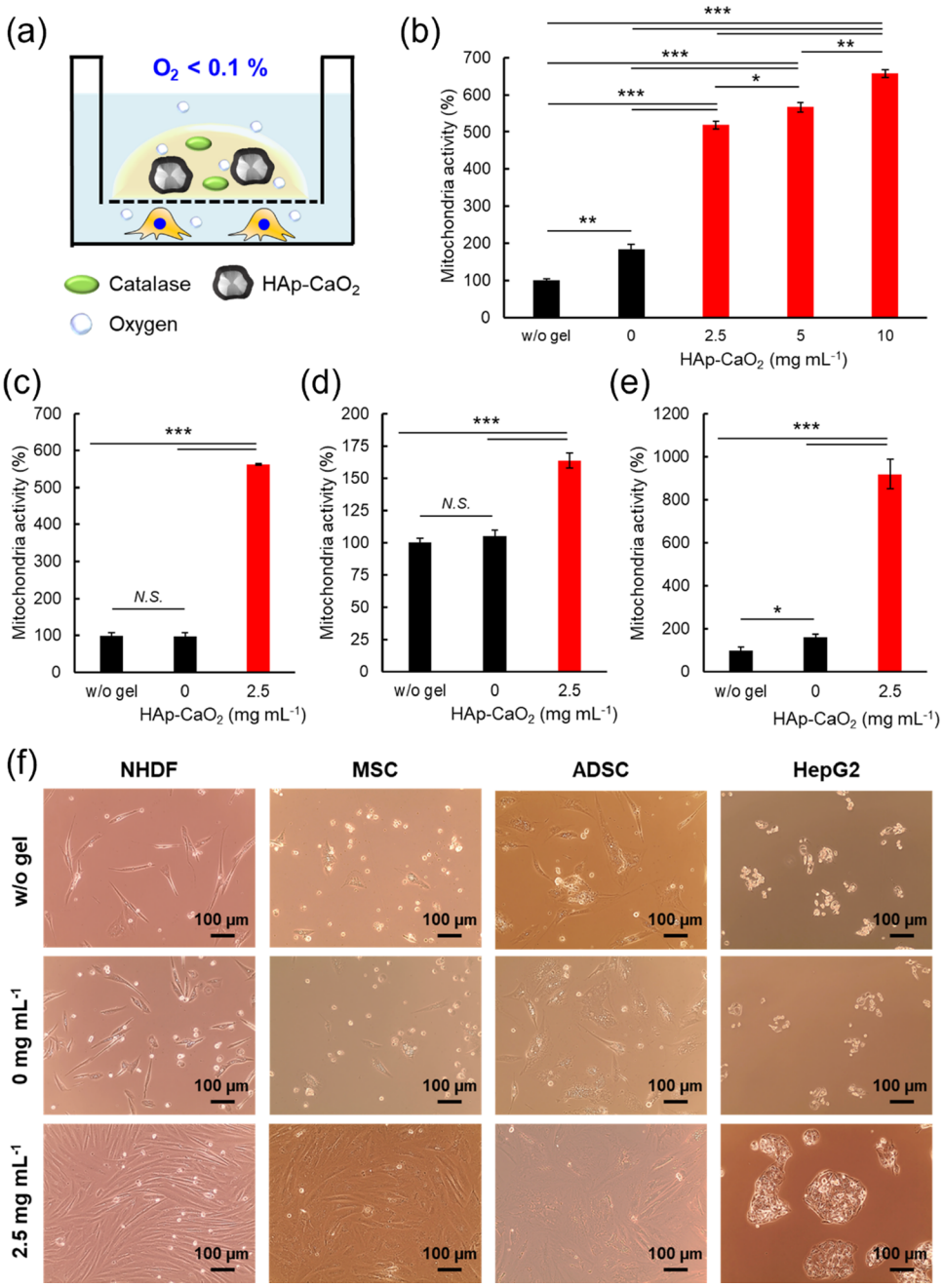

Figure 6. (a) Schematic illustration of the cell culture using an oxygen-releasing hydrogel under a hypoxic condition. The mitochondrial activity of (b) NHDF, (c) MSC, (d) ADSC, and (e) HepG2 and (f) phase contrast images of each sample after 7 days incubation with hydrogels including 100 U mL^{-1} catalase and various concentrations of HAp-CaO_2 (500 mM PB) under a hypoxic condition. The mitochondrial activity of each sample was standardized from the relative values as compared to 100% for that of a cell culture without a hydrogel. All data are representative of three independent experiments, mean ± SD. *p < 0.05, **p < 0.01, and ***p < 0.001.

hydrogen peroxide was decomposed by the components of DMEM such as methionine.[47] On the other hand, hydrogen peroxide was hardly detected in any of the hydrogels with catalase (H_2O_2 <1.5 μM) because catalase is an enzyme that decomposes hydrogen peroxide into oxygen. These results clearly suggested that potentially cytotoxic hydrogen peroxide release from hydrogels is dramatically suppressed using catalase.

Accordingly, we used hydrogels including catalase for further characterization as preparation for cell culture experiments (see Section 3.4). In addition to hydrogen peroxide, $Ca(OH)_2$ is also released as a by-product of the CaO_2 reaction. Since $Ca(OH)_2$ is a basic substrate, pH changes of DMEM with hydrogels were evaluated. As shown in Figure S7, the pH value did not change for 5 days even in the hydrogel including 10 mg mL^{-1} HAp-CaO_2 (100 mM PB), suggesting that the influence of $Ca(OH)_2$ is negligible.

The time span over which oxygen is released is one of the most important properties of oxygen-releasing materials. To evaluate the oxygen release behavior of hydrogels, dissolved oxygen concentrations in DMEM with hydrogels were evaluated under a hypoxia condition (O_2 <0.1%). At first, the oxygen release behavior of hydrogels including 2.5 mg mL^{-1} uncoated CaO_2 or HAp-CaO_2 prepared by 100 and 500

https://doi.org/10.1021/acs.chemmater.3c00601
Chem. Mater. 2023, 35, 5378−5391

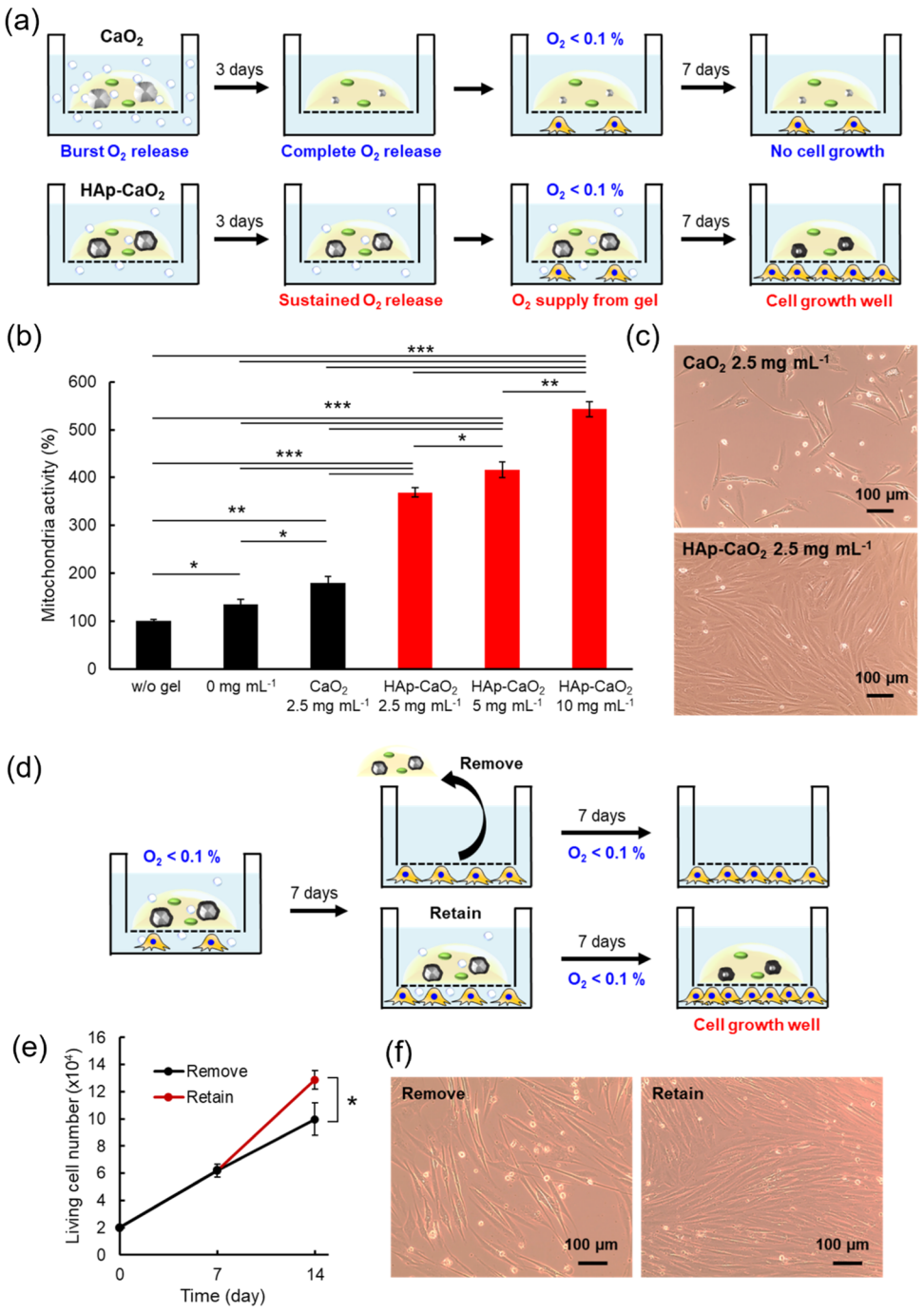

Figure 7. (a) Schematic illustration of the 7-day cell culture under a hypoxic condition using 3 days of preincubated oxygen-releasing hydrogels including CaO_2 or HAp-CaO_2. (b) Mitochondrial activity and (c) phase contrast images of NHDF after 7 days incubation under a hypoxic condition with 3 days preincubated hydrogels including 100 U mL^{-1} catalase and 2.5 mg mL^{-1} CaO_2 or various concentrations of HAp-CaO_2 (500 mM PB). The mitochondrial activity of each sample was standardized from the relative values as compared to 100% for that of a cell culture without a hydrogel. (d) Schematic illustration of the 14-day cell culture under a hypoxic condition using oxygen-releasing hydrogels. Hydrogels were removed or retained after 7 days of incubation. (e) Living cell number of NHDF after 7 and 14 days of incubation under a hypoxic condition using a hydrogel including 100 U mL^{-1} catalase and 10 mg mL^{-1} HAp-CaO_2. The hydrogel was removed or retained and medium was changed to a fresh one after 7 days of incubation. (f) Phase contrast images of NHDF after 14 days of incubation under a hypoxic condition using the oxygen-releasing hydrogel. All data are representative of three independent experiments, mean ± SD. *$p < 0.05$, **$p < 0.01$, and ***$p < 0.001$.

mM PB was measured to evaluate the effect of the HAp coating on CaO_2 microparticles (Figure 5b,c). As expected, the hydrogel including uncoated CaO_2 showed an initial burst release of oxygen and short-term oxygen release for only 3 days due to the rapid reaction with water. On the other hand, in the case of the hydrogel including HAp-CaO_2 by 100 mM PB, the initial burst release of oxygen was suppressed compared to uncoated CaO_2 and the oxygen release period increased to 4 days. In addition, the hydrogel including HAp-CaO_2 by 500 mM PB showed a drastic suppression of the initial burst release of oxygen and the long-term oxygen release of around 10 days. These results clearly confirmed that PB concentration-

https://doi.org/10.1021/acs.chemmater.3c00601
Chem. Mater. 2023, 35, 5378−5391

dependent HAp coating on CaO_2 microparticles suppressed the reaction with water, which enabled sustained oxygen release from the hydrogel. Furthermore, when HAp-CaO_2 (500 mM PB) concentration in the hydrogels increased from 0 to 10 mg mL^{-1}, the dissolved oxygen concentration also increased (Figure 5d,e). For example, dissolved oxygen concentrations after 5 days of incubation were 6.0% (2.5 mg mL^{-1}), 8.8% (5 mg mL^{-1}), and 15.2% (10 mg mL^{-1}). Since the dissolved oxygen concentration in the real tissue such as the heart (9−18%), skeletal muscle (9−18%), brain (16%), and liver (19−28%) is similar to these values,[48] the oxygen-releasing properties of these hydrogels should be sufficient for tissue engineering application.

3.4. Cell Culture with Oxygen-Releasing Hydrogels under a Hypoxic Condition. To evaluate the effect of oxygen supply from the hydrogels on cell proliferation, normal human dermal fibroblast (NHDF) was cultured with oxygen-releasing hydrogels including HAp-CaO_2 (500 mM PB) under a hypoxic condition (O_2 <0.1%) (Figure 6a). After 7 days of incubation, the mitochondrial activity of each sample was assessed by the WST assay because the mitochondrial function is closely related to oxygen.[49] To easily compare cell proliferation, the relative values of mitochondrial activity as compared to 100% for that of a cell culture without a hydrogel are shown in Figure 6b. In the case of the hydrogel without HAp-CaO_2, mitochondrial activity increased slightly, probably because oxygen originally dissolving in the hydrogel was supplied to the cells in the early stages of incubation. On the other hand, the hydrogel including 2.5 mg mL^{-1} HAp-CaO_2 showed dramatically increased mitochondrial activity to 518%. Furthermore, as the HAp-CaO_2 concentration in the hydrogels increased from 2.5 to 5 and 10 mg mL^{-1}, mitochondrial activity also increased from 518 to 567 and 657%. This result is consistent with the trend that the amount of released oxygen increased with HAp-CaO_2 concentration in the hydrogels (Figure 5d,e). In addition to NHDF, mesenchymal stem cells (MSCs) (Figure 6c), adipose-derived stem cells (ADSCs) (Figure 6d), and HepG2 (Figure 6e) cells were also cultured with oxygen-releasing hydrogels under a hypoxic condition. Although the ADSC is often used for regenerative medicine of adipose tissue reconstruction, transplantation of adipose tissues is unsuitable for tissue reconstruction as the lack of blood vessels results in inadequate nutrient and oxygen delivery, leading to necrosis *in situ*.[50] The oxygen-releasing hydrogel including 2.5 mg mL^{-1} HAp-CaO_2 showed increased mitochondrial activity to 563% for MSC, 164% for ADSC, and 920% for HepG2. These differences in mitochondrial activity are probably because of the differences in oxygen utilization for each cell.[51] Cell morphologies of each sample after 7 days of incubation under a hypoxic condition are shown in phase contrast images (Figure 6f). The cells did not spread well without oxygen-releasing hydrogels probably because the lack of oxygen affected cell function.[52] On the other hand, the cells spread and proliferated very well with oxygen-releasing hydrogels. According to these results, it is confirmed that the oxygen supply from hydrogels improved cell proliferation of various cell types under a hypoxic condition.

As shown in Figure 5, a HAp coating on CaO_2 dramatically increased the oxygen release periods of hydrogels. Thus, to evaluate the effects of the HAp coating on CaO_2 for cell proliferation, NHDF was cultured with preincubated hydrogels including uncoated CaO_2 or HAp-CaO_2 under a hypoxic condition. Since the oxygen release period of the hydrogel including uncoated CaO_2 is only 3 days (Figure 5b,c), oxygen release from the hydrogel should be completed within 3 days of preincubation in DMEM. On the other hand, since the oxygen release period of the hydrogel including HAp-CaO_2 is 10 days, an additional 7 days of oxygen release is expected even after 3 days of preincubation, which is expected to improve cell proliferation under a hypoxic condition (Figure 7a). Hydrogels including 2.5 mg mL^{-1} HAp-CaO_2 dramatically increased mitochondrial activity to 369%, while it was only 180% for the hydrogel including 2.5 mg mL^{-1} uncoated CaO_2 (Figure 7b). In addition, phase contrast images after 7 days of cell culture confirmed marked cell proliferation only in the hydrogel including HAp-CaO_2 (Figure 7c). These results clearly confirmed that the HAp coating on CaO_2 achieved sustained oxygen release from the hydrogel, which dramatically improved cell proliferation under a hypoxic condition compared to that of uncoated CaO_2. Furthermore, similar to the case shown in Figure 6b, as the HAp-CaO_2 concentration in the hydrogels increased from 2.5 to 5 and 10 mg mL^{-1}, mitochondrial activity also increased from 369 to 416 and 543%. This is also probably because the amount of released oxygen increased with HAp-CaO_2 concentration in the hydrogels (Figure 5d,e).

To evaluate the longer-term effects of oxygen-releasing hydrogels on cells, NHDF was cultured with the oxygen-releasing hydrogel including 10 mg mL^{-1} HAp-CaO_2 for 2 weeks under a hypoxic condition. After 7 days of cell culture with oxygen-releasing hydrogels, the hydrogels were removed or retained (Figure 7d). After an additional 7 days of cell culture under a hypoxic condition, the living cell number was assessed by trypan blue (Figure 7e). During the first 7 days of cell culture, the living cell number increased from 2.0×10^4 to 6.2×10^4 because of the oxygen supply from the hydrogel. In the case where the hydrogel was removed, the living cell number increased from 6.2×10^4 to 10.0×10^4 during the additional 7 days of cell culture. When the hydrogel was removed, the culture medium was also changed to a fresh one. Thus, it is expected that because of the oxygen supply from the fresh medium, the cell number increased even without a hydrogel. Importantly, in the case where the hydrogel was retained, the living cell number increased from 6.2×10^4 to 12.9×10^4 during the additional 7 days of cell culture. Since the living cell number at 14 days is statistically significant compared to the case where the hydrogel was removed, the contribution of oxygen supply from the hydrogel is clearly suggested. Phase contrast images after 14 days of cell culture also suggested cell proliferation when the hydrogel was retained (Figure 7f). These results confirmed that sustained oxygen supply from the hydrogel including HAp-CaO_2 improved cell proliferation even after 7 days of cell culture.

3.5. Construction of the 3D Tissue in the Presence of the Oxygen-Releasing Hydrogel. To evaluate the effect of oxygen supply from the hydrogels on the construction of a thick 3D tissue, the 3D tissue was fabricated using mouse L929 fibroblast cells in the presence of the oxygen-releasing hydrogel, as shown in Figure S8a. It is already reported that limited diffusion of oxygen causes cell death inside the L929 tissues.[53] After 3 days of tissue culture in the absence or presence of the oxygen-releasing hydrogel, the morphology of the constructed 3D tissue was investigated by HE staining. In the absence of the hydrogel, the HE staining image showed many gaps in the 3D tissue, suggesting cell death due to oxygen shortage (Figure S8b). On the other hand, in the presence of the oxygen-releasing hydrogel, the HE staining

https://doi.org/10.1021/acs.chemmater.3c00601
Chem. Mater. 2023, 35, 5378−5391

image showed a thick 3D tissue with high cell density (Figure S8c). For the quantitative evaluation, cell densities around the center area were calculated from HE staining images. Compared to the tissue culture in the absence of the hydrogel, cell density was significantly higher in the presence of the oxygen-releasing hydrogel (Figure S8d). Furthermore, fluorescence images showed that the fluorescence derived from actin (red) is stronger in the presence of the oxygen-releasing hydrogel (Figure S8e). These results clearly suggested that oxygen supply from the hydrogels relieved oxygen shortage in the 3D tissue, which improved cell viability in the 3D tissue.

4. CONCLUSIONS

This study introduces a simple strategy to prepare HAp-coated CaO_2 microparticles just by immersing CaO_2 in PB. Since the HAp coating on CaO_2 acts as a diffusion barrier and thus delays the reaction with water, both the usual initial burst release of oxygen was suppressed and a sustained oxygen release behavior was achieved. In addition, there was a clear relationship between the HAp amount of CaO_2 and PB concentration, which enabled PB concentration-dependent oxygen release from CaO_2. Since HAp coating on CaO_2 microparticles is a very simple procedure and highly effective for sustained oxygen release, the application of this novel method to existing or yet-to-be-developed oxygen-releasing materials is greatly anticipated.

We demonstrate this with the example of gelatin hydrogels, one of the most applied hydrogel materials in tissue engineering. Oxygen-releasing gelatin hydrogels enzymatically cross-linked by TG were successfully fabricated using catalase and HAp-CaO_2 because the HAp coating on CaO_2 suppressed the burst release of hydrogen peroxide, which inactivated TG. Hydrogels cross-linked by enzymatic reactions are highly biocompatible and often applied for *in vitro*/*vivo* experiments. Thus, HAp-CaO_2 provides a broader range of material designs for oxygen-releasing materials. Hydrogels including HAp-CaO_2 released oxygen for 10 days compared to only 3 days for the hydrogel including uncoated CaO_2. In the previous study, Shen and co-workers reported 6 days of oxygen release from oxygen-releasing polycaprolactone/CaO_2 composite microspheres with a diameter of around 25 μm.[24] Recently, Leijten and co-workers reported 12 days of oxygen release from the gelatin methacryloyl hydrogel containing polycaprolactone/CaO_2 composite microspheres with a diameter of around 5 μm.[23] Therefore, the oxygen release period of our system is comparable to that of previously reported oxygen-releasing materials using hydrophobic polymers. In addition, Akashi and co-workers reported the transplantation of 3D artificial human vascular tissues with a thickness of around 50 μm and they showed that the implanted artificial human vascular networks were connected to the host blood vessel within 2 weeks after the transplantation.[54] Therefore, if 3D tissues with oxygen-releasing scaffolds including HAp-CaO_2 are transplanted, suppression of cell death due to oxygen shortage is expected by 10 days of oxygen supply before the connection to the host blood vessel. Since HAp-CaO_2 microparticles can be incorporated in any substrates, it is also expected that incorporation of HAp-CaO_2 in hydrophobic polymers enables a much longer sustained oxygen supply from the biomaterials, which will relieve hypoxia conditions for a much longer time. *In vitro* experiments confirmed that sustained oxygen supply from our hydrogels improved the proliferation of various cell types under a hypoxic condition. Therefore, we propose that HAp-CaO_2 and these oxygen-releasing hydrogels show great potential for solving the oxygen shortage problem in regenerative medicine and tissue engineering fields.

■ ASSOCIATED CONTENT

Supporting Information

The Supporting Information is available free of charge at https://pubs.acs.org/doi/10.1021/acs.chemmater.3c00601.

Additional data analysis includes the dissolution behavior of CaO_2, hydrogen peroxide release behavior of CaO_2, SEM images of HAp-CaO_2, hydrogel properties, pH changes of hydrogels, and construction of the 3D tissue in the presence of the oxygen-releasing hydrogel (PDF)

Movie S1 (MP4)

Movie S2 (MP4)

■ AUTHOR INFORMATION

Corresponding Author

Michiya Matsusaki − *Division of Applied Chemistry, Graduate School of Engineering, Osaka University, Suita, Osaka 565-0871, Japan;* orcid.org/0000-0003-4294-9313; Email: m-matsus@chem.eng.osaka-u.ac.jp

Authors

Daisuke Tomioka − *Division of Applied Chemistry, Graduate School of Engineering, Osaka University, Suita, Osaka 565-0871, Japan; AIST-Osaka University Advanced Photonics and Biosensing Open Innovation Laboratory, National Institute of Advanced Industrial Science and Technology (AIST), Suita, Osaka 565-0871, Japan*

Satoshi Fujita − *AIST-Osaka University Advanced Photonics and Biosensing Open Innovation Laboratory, National Institute of Advanced Industrial Science and Technology (AIST), Suita, Osaka 565-0871, Japan*

Jürgen Groll − *Department for Functional Materials in Medicine and Dentistry at the Institute of Functional Materials and Biofabrication and Bavarian Polymer Institute, University of Würzburg, D-97070 Würzburg, Germany;* orcid.org/0000-0003-3167-8466

Complete contact information is available at: https://pubs.acs.org/10.1021/acs.chemmater.3c00601

Author Contributions

D.T. carried out the experiments. D.T. wrote the manuscript. All authors edited the manuscript. All authors contributed to the design and implementation of the research and the analysis of results. All authors have seen and approved the final manuscript.

Notes

The authors declare no competing financial interest.

■ ACKNOWLEDGMENTS

The authors acknowledge Profs. T. Kida and H. Uyama at Osaka University for XRD and SEM-EDX analyses, respectively. The authors also thank Prof. Y. Sowa at Kyoto University and Prof. L. Fiona at Osaka University for the kind donation of ADSC. This study was financially supported by the Mirai-Program (18077228) from JST, JPNP20004 from NEDO, the Grant-in-Aid for Scientific Research (A) (20H00665), the Grant-in-Aid for Challenging Exploratory Research (22K19918), the Grant-in-Aid for JSPS Fellows

https://doi.org/10.1021/acs.chemmater.3c00601
Chem. Mater. 2023, 35, 5378−5391

(A22J205330) from JSPS, and the Bilateral project between JSPS and DAAD (JPJSBP120213505). The English proof of this manuscript was financially supported by the Grant-in-Aid for JSPS Fellows (A22J205330) from JSPS.

REFERENCES

(1) Shimizu, T.; Hidekazu, S.; Joseph, Y.; Yuki, I.; Masayuki, Y.; Akihiro, K.; Eiji, K.; Teruo, O. Polysurgery of cell sheet grafts overcomes diffusion limits to produce thick, vascularized myocardial tissues. *FASEB J.* **2006**, *20*, 708−710.
(2) Jain, R. K.; Patrick, A.; Josh, T.; Dan, G. D.; Dai, F. Engineering vascularized tissue. *Nat. Biotechnol.* **2005**, *23*, 821−823.
(3) Radisic, M.; Jos, M.; Eric, E.; Wenliang, G.; Robert, L.; Gordana, V. N. Oxygen gradients correlate with cell density and cell viability in engineered cardiac tissue. *Biotechnol. Bioeng.* **2006**, *93*, 332−343.
(4) Mizukami, Y.; Yuki, T.; Kazunori, S.; Satoshi, K.; Yoshinobu, T.; Makiya, N. Calcium Peroxide-Containing Polydimethylsiloxane-Based Microwells for Inhibiting Cell Death in Spheroids through Improved Oxygen Supply. *Biol. Pharm. Bull.* **2021**, *44*, 1458−1464.
(5) Willemen, N. G.; Shabir, H.; Melvin, G.; Jinghang, L.; Iris, E. A.; Su, R. S.; Jeroen, L. Oxygen-Releasing Biomaterials: Current Challenges and Future Applications. *Trends Biotechnol.* **2021**, *39*, 1144−1159.
(6) Farris, A. L.; Alexandra, N. R.; Warren, L. G. Oxygen Delivering Biomaterials for Tissue Engineering. *J. Mater. Chem. B* **2016**, *4*, 3422−3432.
(7) Agarwal, T.; Sara, K.; Marco, C.; Francisca, P.; Clara, R. C.; Vitor, G.; Leila, M.; Carmelo, D. M.; Joao, F. M.; Massoud, V.; Pooyan, M.; Tapas, K. M. Oxygen releasing materials: Towards addressing the hypoxia-related issues in tissue engineering. *Mater. Sci. Eng. C* **2021**, *122*, No. 111896.
(8) Paciello, A.; Giuseppe, A.; Alessandro, G.; Francesco, U.; Paolo, A. N. Hemoglobin-Conjugated Gelatin Microsphere as a Smart Oxygen Releasing Biomaterial. *Adv. Healthcare Mater.* **2016**, *5*, 2655−2666.
(9) Ohta, S.; Kenichiro, H.; Xiaoting, F.; Masamichi, K.; Yasuyuki, S.; Taichi, I. Development of human-derived hemoglobin-albumin microspheres as oxygen carriers using Shirasu porous glass membrane emulsification. *J. Biosci. Bioeng.* **2018**, *126*, 533−539.
(10) Tomioka, D.; Hirotaka, N.; Shigeru, M.; Yoshiki, S.; Michiya, M. Development of temperature dependent oxygen releasable nanofilm by modulating oxidation state of myoglobin. *Chem. Commun.* **2021**, *57*, 5131−5134.
(11) Kishimura, A.; Aya, K.; Kensuke, O.; Yuichi, Y.; Kazunori, K. Encapsulation of Myoglobin in PEGylated Polyion Complex Vesicles Made from a Pair of Oppositely Charged Block Ionomers: A Physiologically Available Oxygen Carrier. *Angew. Chem., Int. Ed.* **2007**, *46*, 6085−6088.
(12) Yao, Y.; Minmin, Z.; Tian, L.; Juan, Z.; Yuan, G.; Zhengfeng, W.; Jun, G.; Jun, Z.; Zhaofen, L.; Dannong, H. Perfluorocarbon-Encapsulated PLGA-PEG Emulsions as Enhancement Agents for Highly Efficient Reoxygenation to Cell and Organism. *ACS Appl. Mater. Interfaces* **2015**, *7*, 18369−18378.
(13) Fu, X.; Seiichi, O.; Masamichi, K.; Yasuyuki, S.; Taichi, I. Size-Controlled Preparation of Microsized Perfluorocarbon Emulsions as Oxygen Carriers via the Shirasu Porous Glass Membrane Emulsification Technique. *Langmuir* **2019**, *35*, 4094−4100.
(14) Lee, H.-Y.; Hae, W. K.; Jin, H. L.; Se, H. O. Controlling oxygen release from hollow microparticles for prolonged cell survival under hypoxic environment. *Biomaterials* **2015**, *53*, 583−591.
(15) Wang, H.; Yongsheng, Z.; Tianyi, L.; Zhen, C.; Yinan, W.; Chuanyu, Q. Properties of calcium peroxide for release of hydrogen peroxide and oxygen: A kinetics study. *Chem. Eng. J.* **2016**, *303*, 450−457.
(16) Park, S.; Kyung, M. P. Hyperbaric oxygen-generating hydrogels. *Biomaterials* **2018**, *182*, 234−244.
(17) Alemdar, N.; Jeroen, L.; Gulden, C. U.; Jesper, H.; Joao, R.; Arghya, P.; Pooria, M.; Akhilesh, K. G.; Yiling, Q.; Sameer, S.; Ronglih, L.; Ali, K. Oxygen-Generating Photo-Cross-Linkable Hydrogels Support Cardiac Progenitor Cell Survival by Reducing Hypoxia-Induced Necrosis. *ACS Biomater. Sci. Eng.* **2017**, *3*, 1964−1971.
(18) Newland, B.; Marcel, B.; Dimitri, E.; Heike, N.; Carsten, W. Oxygen-Producing Gellan Gum Hydrogels for Dual Delivery of Either Oxygen or Peroxide with Doxorubicin. *ACS Biomater. Sci. Eng.* **2017**, *3*, 787−792.
(19) Mehrotra, S.; Rishabh, D. S.; Ashutosh, B.; Janani, G.; Souradeep, D.; Biman, B. M. Engineering Microsphere-Loaded Non-mulberry Silk-Based 3D Bioprinted Vascularized Cardiac Patches with Oxygen-Releasing and Immunomodulatory Potential. *ACS Appl. Mater. Interfaces* **2021**, *13*, 50744−50759.
(20) Pedraza, E.; Maria, M. C.; Christopher, A. F.; Camillo, R.; Cherie, L. S. Preventing hypoxia-induced cell death in beta cells and islets via hydrolytically activated, oxygen-generating biomaterials. *Proc. Natl. Acad. Sci. U.S.A.* **2012**, *109*, 4245−4250.
(21) Liang, J.-P.; Robert, P. A.; Madhuvanthi, S.; Amy, E.; Maria, M. C.; Cherie, L. S. Engineering a macroporous oxygen-generating scaffold for enhancing islet cell transplantation within an extrahepatic site. *Acta Biomater.* **2021**, *130*, 268−280.
(22) Daneshmandi, L.; Cato, T. L. Regenerative engineered vascularized bone mediated by calcium peroxide. *J. Biomed. Mater. Res., Part A* **2020**, *108*, 1045−1057.
(23) Farzin, A.; Shabir, H.; Liliana, S. M. T.; Melvin, G.; Joao, F. C.; Varun, M.; Aurelie, C.; Hojae, B.; Liesbet, G.; Iman, N.; Su, R. S.; Leijten, J. Self-Oxygenation of Tissues Orchestrates Full-Thickness Vascularization of Living Implants. *Adv. Funct. Mater.* **2021**, *31*, No. 2100850.
(24) Zhang, M.; Tawan, K.; Shen, W. Oxygen-releasing polycaprolactone/calcium peroxide composite microspheres. *J. Biomed. Mater. Res., Part B* **2020**, *108*, 1097−1106.
(25) Touri, M.; Fathollah, M.; Noor, A. A. O.; Mohammad, M. D.; Peiman, B. M.; Saeed, F. M.; Masoud, M. Oxygen-Releasing Scaffolds for Accelerated Bone Regeneration. *ACS Biomater. Sci. Eng.* **2020**, *6*, 2985−2994.
(26) Mondal, D.; May, G.; Subbu, S. V. Polycaprolactone-based biomaterials for tissue engineering and drug delivery: Current scenario and challenges. *Int. J. Polym. Mater. Polym. Biomater.* **2016**, *65*, 255−265.
(27) Sadat-Shojai, M.; Mohammad, T. K.; Ehsan, D. K.; Ahmad, J. Synthesis methods for nanosized hydroxyapatite with diverse structures. *Acta Biomater.* **2013**, *9*, 7591−7621.
(28) Prakash, K. H.; Kumar, R.; Ooi, C. P.; Cheang, P.; Khor, K. A. Apparent solubility of hydroxyapatite in aqueous medium and its influence on the morphology of nanocrystallites with precipitation temperature. *Langmuir* **2006**, *22*, 11002−11008.
(29) Bhat, S.; Uthappa, U. T.; Tariq, A.; Ho, Y. J.; Mahaveer, D. K. Functionalized Porous Hydroxyapatite Scaffolds for Tissue Engineering Applications: A Focused Review. *ACS Biomater. Sci. Eng.* **2022**, *8*, 4039−4076.
(30) Shuai, C.; Bo, P.; Pei, F.; Li, Y.; Ruilin, L.; Anjie, M. In situ synthesis of hydroxyapatite nanorods on graphene oxide nanosheets and their reinforcement in biopolymer scaffold. *J. Adv. Res.* **2022**, *35*, 13−24.
(31) Feng, P.; Kai, W.; Yang, S.; Shuping, P.; Yongbin, H.; Cijun, S. Hydroxyapatite nanoparticles in situ grown on carbon nanotube as a reinforcement for poly (ε-caprolactone) bone scaffold. *Mater. Today Adv.* **2022**, *15*, No. 100272.
(32) Shuai, C.; Wenjing, Y.; Pei, F.; Shuping, P.; Hao, P. Accelerated degradation of HAP/PLLA bone scaffold by PGA blending facilitates bioactivity and osteoconductivity. *Bioact. Mater.* **2021**, *6*, 490−502.
(33) Lorand, L.; Robert, M. G. Transglutaminases: crosslinking enzymes with pleiotropic functions. *Nat. Rev. Mol. Cell Biol.* **2003**, *4*, 140−156.
(34) Yang, G.; Zhenghua, X.; Xiaomei, R.; Haiyan, L.; Hong, Q.; Kunlong, M.; Yingqiang, G. Enzymatically crosslinked gelatin hydrogel promotes the proliferation of adipose tissue-derived stromal cells. *PeerJ* **2016**, *4*, No. e2497.

https://doi.org/10.1021/acs.chemmater.3c00601
Chem. Mater. 2023, 35, 5378−5391

(35) Zhou, Y.; Shenglong, L.; Yanji, C.; Bin, Y.; Xinglei, T.; Xiaohua, H.; Yapei, W. An injectable bioink with rapid prototyping in the air and *in-situ* mild polymerization for 3D bioprinting. *Biofabrication* **2021**, *13*, No. 045026.
(36) Affolter-Zbaraszczuk, C.; Hayriye, O.; Florent, M.; Olivier, G.; Philippe, L.; Vincent, Ball.; Camelia, M. G.; Pierre, S.; Helena, K. M. Hybrid extracellular matrix microspheres for development of complex multicellular architectures. *RSC Adv.* **2017**, *7*, 5528−5532.
(37) Xu, Y.; Raphael, P. B. J.; Yi, S.; Daniele, V.; David, M.; Shuyuan, Z.; Tuomas, P. J. K. Microfluidic Templating of Spatially Inhomogeneous Protein Microgels. *Small* **2020**, *16*, No. 2000432.
(38) Alfonso-Prieto, M.; Xevi, B.; Pietro, V.; Carme, R. The molecular mechanism of the catalase reaction. *J. Am. Chem. Soc.* **2009**, *131*, 11751−11761.
(39) Han, T. J. An improved phosphorus assay for oils without carcinogenic hydrazine sulfate. *J. Am. Oil Chem. Soc.* **1995**, *72*, 881−885.
(40) Matsusaki, M.; Takashi, K.; Tetsuro, S.; Jun-ichi, K.; Akio, K.; Mitsuru, A. Novel Guglielmi detachable coils (GDCs) for the treatment of brain aneurysms. In vitro study of hydroxyapatite coating on Pt plate as GDCs model. *J. Biomed. Mater. Res., Part B* **2003**, *66*, 429−438.
(41) Louis, F.; Yoshihiro, S.; Shiro, K.; Michiya, M. High-throughput drug screening models of mature adipose tissues which replicate the physiology of patients' Body Mass Index (BMI). *Bioact. Mater.* **2022**, *7*, 227−241.
(42) Li, X.; Yanhua, X.; Fei, J.; Bo, W.; Qili, H.; Yong, T.; Ting, L.; Tong, W. Enhanced phosphate removal from aqueous solution using resourceable nano-CaO_2/BC composite: Behaviors and mechanisms. *Sci. Total Environ.* **2020**, *709*, No. 136123.
(43) Haider, A.; Sajjad, H.; Sung, S. H.; Inn, K. K. Recent advances in the synthesis, functionalization and biomedical applications of hydroxyapatite: a review. *RSC Adv.* **2017**, *7*, 7442−7458.
(44) Koutsopoulos, S. Synthesis and characterization of hydroxyapatite crystals: a review study on the analytical methods. *J. Biomed. Mater. Res.* **2002**, *62*, 600−612.
(45) Nagul, E. A.; Ian, D. M.; Paul, W.; Spas, D. K. The molybdenum blue reaction for the determination of orthophosphate revisited: Opening the black box. *Anal. Chim. Acta* **2015**, *890*, 60−82.
(46) Yi, M. C.; Arek, V. M.; James, A. O.; Chaitan, K. Endoplasmic reticulum-resident protein 57 (ERp57) oxidatively inactivates human transglutaminase 2. *J. Biol. Chem.* **2018**, *293*, 2640−2649.
(47) Boonvisut, S.; Anders, A.; Leif, R. N. Oxidation of methionine. Effects of hydrogen peroxide alone and in combination with iodide and selenite. *Food Chem.* **1982**, *9*, 183−194.
(48) De Santis, V.; Singer, M. Tissue oxygen tension monitoring of organ perfusion: rationale, methodologies, and literature review. *Br. J. Anaesth.* **2015**, *115*, 357−365.
(49) Zhang, H.; Marta, B. M.; Larissa, A. S.; Yee, S. T.; Jin, H. B.; Jacob, B. W.; Frank, J. G.; Gregg, L. S. Mitochondrial Autophagy Is an HIF-1-dependent Adaptive Metabolic Response to Hypoxia. *J. Biol. Chem.* **2008**, *283*, 10892−10903.
(50) Karanfil, A. S.; Fiona, L.; Michiya, M. Biofabrication of vascularized adipose tissues and their biomedical applications. *Mater. Horiz.* **2023**, *10*, 1539−1558.
(51) Wagner, B. A.; Sujatha, V.; Garry, R. B. The rate of oxygen utilization by cells. *Free. Radical Biol. Med.* **2011**, *51*, 700−712.
(52) Sendoel, A.; Michael, O. H. Apoptotic cell death under hypoxia. *Physiology* **2014**, *29*, 168−176.
(53) Neto, A. I.; Correia, C. R.; Oliveira, M. B.; Rial-Hermida, M. I.; Alvarez-Lorenzo, C.; Reis, R. L.; Mano, J. F. A novel hanging spherical drop system for the generation of cellular spheroids and high throughput combinatorial drug screening. *Biomater. Sci.* **2015**, *3*, 581−585.
(54) Asano, Y.; Hiroshi, S.; Daisuke, O.; Michiya, M.; Akashi, M. Transplantation of three-dimensional artificial human vascular tissues fabricated using an extracellular matrix nanofilm-based cell accumulation technique. *J. Tissue Eng. Regen. Med.* **2017**, *11*, 1303−1307.

https://doi.org/10.1021/acs.chemmater.3c00601
Chem. Mater. 2023, 35, 5378−5391